Mechanism of Solid/Liquid Interfacial Reactions. Atomic Force Microscopy Studies of the Self-Passivating Reaction between Solid *p*-Chloranil and Aqueous Phase *N*,*N*-Dimethylphenylenediamine

Jonathan Booth and Richard G. Compton*

Physical and Theoretical Chemistry Laboratory, Oxford University, South Parks Road, Oxford OX1 3QZ, United Kingdom

John H. Atherton

Zeneca Huddersfield Works, P.O. Box A38, Leeds Road, Huddersfield, HD2 1FF, United Kingdom

Received: January 27, 1998

The reaction between solid *p*-chloranil and alkaline aqueous solutions of dimethylphenylenediamine is shown to be self-passivating owing to the formation of insoluble product at the reacting interface. In situ atomic force microscopy imaging of the reaction occurring at (010) surfaces of single crystals of *p*-chloranil show that the nucleation of the overgrowth is progressive and that its coverage, *S*, follows the time (*t*) dependence $S(t) = 1 - \exp(-k_3t^3)$, where k_3 is a rate constant. Measurement of the *z* piezo voltage throughout the reaction to give an absolute measure of the surface height shows that appreciable (hydroxide driven) dissolution occurs prior to the formation of the overgrowth and the surface becoming fully passivated.

Introduction

Chemical reactions between an organic solid and a solution phase reagent are of no little synthetic and industrial importance.[1] In general two mechanistic limits may be recognized; either the solid may dissolve and then react with the solution phase species homogeneously or alternatively the latter may react directly with the solid reagent at the solid/liquid interface. The former behavior was found for the reaction of solid cyanuric chloride with aqueous solutions of amines,[2] where coupling was shown to occur in a thin reaction layer surrounding the dissolving solid but at a rate limited by the dissolution kinetics of the solid. Authentically interfacial solid/liquid reactions are less common but have been demonstrated for the hydrolytic dissolution of triphenylmethyl chloride in water[3] and for the reactive dissolution of *p*-chloranil in basic aqueous solution where the reaction was found to be driven by reaction of the substrate with hydroxide ions at, or very close, to the dissolving surface.[4] A further complication arises when the product of the solid/liquid reaction is insoluble and may present problems to the synthetic chemist if the solid reagent becomes passivated with the product so wasting the former and dictating a possibly difficult and/or expensive separation to recover the latter. Such passivation has been characterized for the reaction of calcium carbonate (as calcite) with sulfuric acid, where insoluble gypsum ($CaSO_4 \cdot 2H_2O$) is formed at the solid/liquid interface and inhibits further acid induced dissolution.[5]

This paper seeks to use atomic force microscopy (AFM) to characterize self-passivating solid/liquid reactions both through the evolution of surface morphology and via kinetic parametrization. In particular attention is focused on the reaction of the (010) plane of single crystals of *p*-chloranil with alkaline aqueous solutions containing *N*,*N*-dimethylphenylenediamine (DMPA, Figure 1). The reaction of halogenils and tetrahalogenated quinones with primary and secondary amines is central to the synthesis of triphenodioxazine dye precursors[6] and the formation of the amine-substituted product is shown schematically in Figure 2. Further reaction takes place to give di- or, in some cases, tetraaminated quinone derivatives.[7] These products display extreme insolubility in aqueous solution[6] so that the system under study represents an ideal but industrially relevant model system with which to study self-passivation processes.

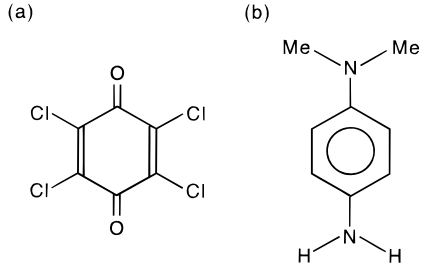

Figure 1. Chemical structures of (a) *p*-chloranil and (b) DMPA.

The kinetic description of the formation of metal films at interfaces using nucleation and growth models is well-developed.[8] In the following we seek to explore whether analogous descriptions can be applied to the formation of deposits formed by chemical reaction at solid/liquid interfaces.

Experimental Section

A Topometrix TMX 2010 Discoverer atomic force microscope, operating in contact mode, was employed to image the surfaces of solid substrates. A commercial Topometrix liquid cell was used, without modification, for in situ AFM imaging. The rates of dissolution of the surfaces of single crystals of *p*-chloranil were measured using the following procedure. First a single crystal was freshly cleaved and imaged in air, typically revealing a smooth (010) surface with a few steps.[4] The smallest steps had an average measured height of 1.08 nm. The same surface was then imaged in an aqueous environment. After slight initial dissolution and roughening of the surface in water

S1089-5647(98)00895-5 CCC: $15.00
Published on Web 04/28/1998

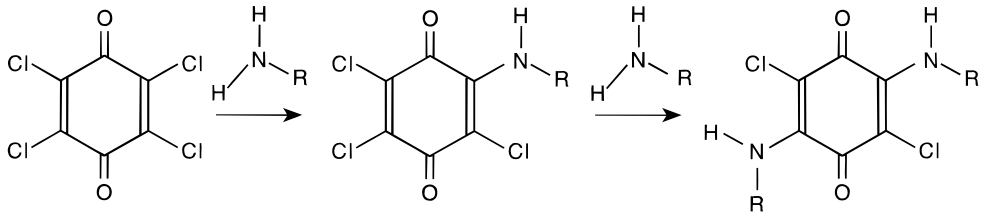

Figure 2. Reaction of a primary amine with a halogenil compound.

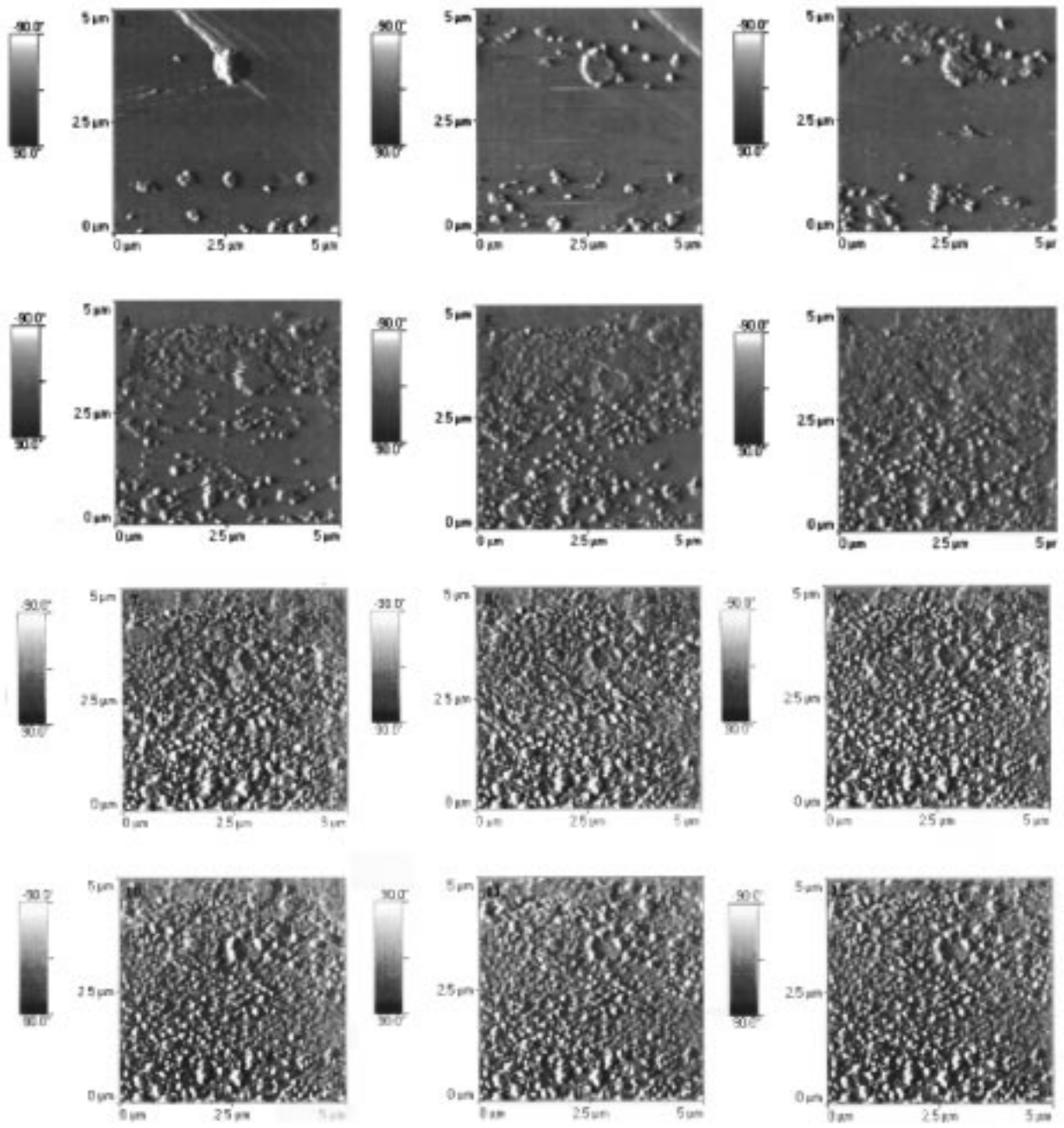

Figure 3. (a, top two rows) AFM sequence showing the passivation of a (010) *p*-chloranil surface on exposure to a solution containing 4.87 mM DMPA, 0.2 M KCl, and 23.8 mM KOH. The first image was recorded after ca. 75 s following solution changeover (see text), and successive images were taken at 25 s intervals. The images are left shaded, and the *z* range varies up to ca. 100 nm. (b, bottom two rows) Continuation of the sequence. Again the time between images is 25 s. The *z* range varies up to ca. 70 nm.

alone at a nominal pH of 7, several images were taken until any drift on the *x*, *y*, and *z* piezo scanner tubes was eliminated and their output steady. Solution containing DMPA was then flowed into the liquid cell, and after ca. 10 mL had passed through the cell, the flow was stopped. Images of the reacting surfaces were recorded continuously, at 25 s intervals, starting approximately 75 s after solution changeover. For quantitative experiments a scan area of 20 × 20 μm was employed. In all cases two sorts of experiment were undertaken: first the recording of conventional topographical images and second the

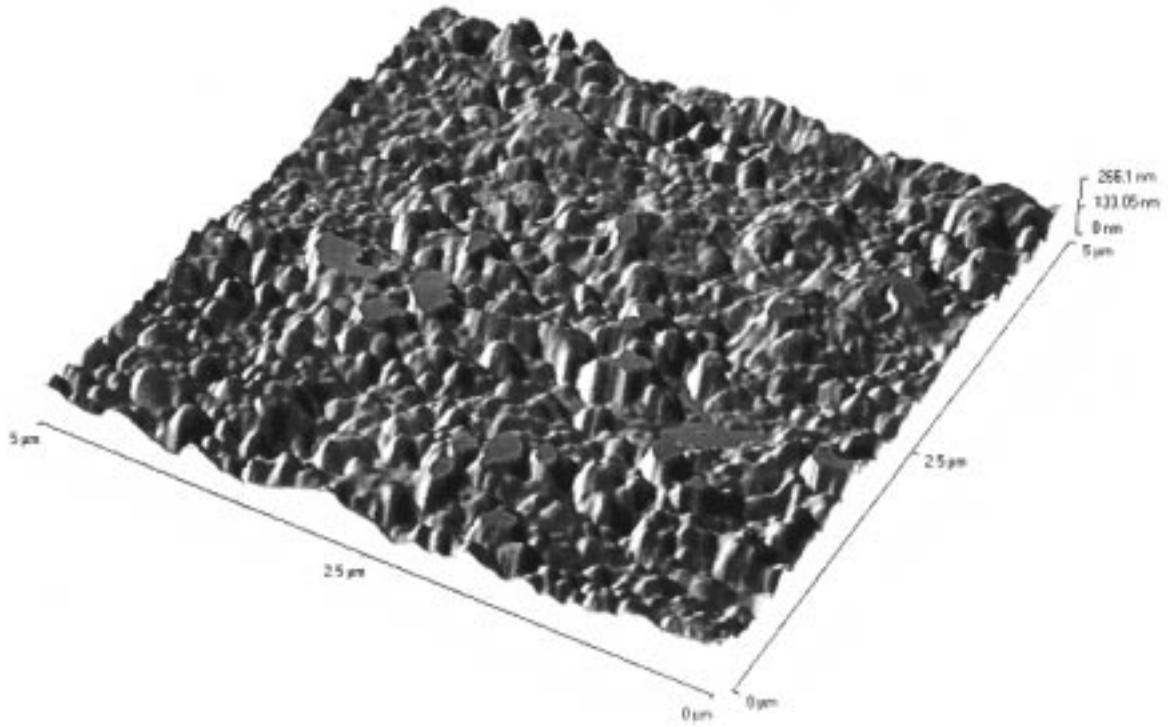

Figure 4. Three-dimensional image of a (010) *p*-chloranil surface after ca. 9.5 min exposure to a solution containing 4.87 mM DMPA, 0.2 M KCl, and 23.8 mM KOH.

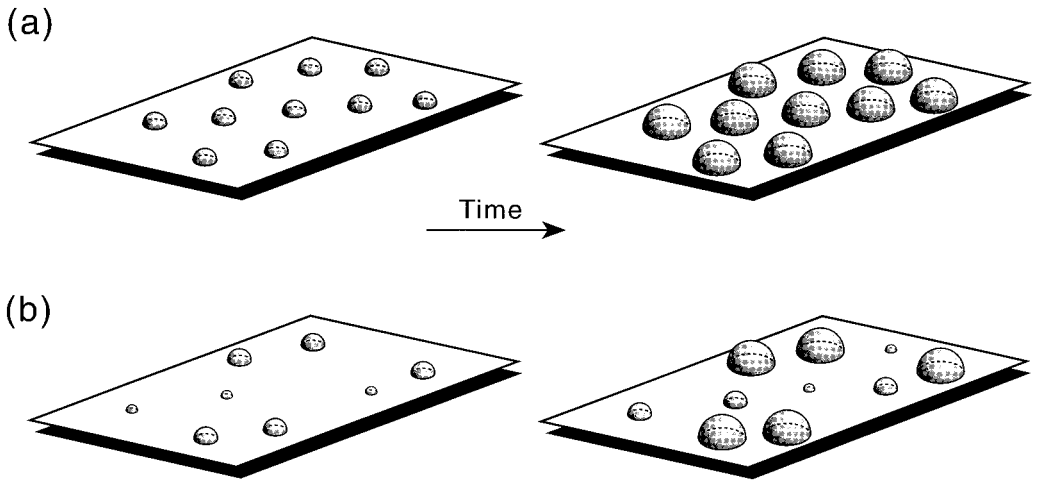

Figure 5. Schematic diagram showing the difference between (a) instantaneous and (b) progressive nucleation of overgrowths.

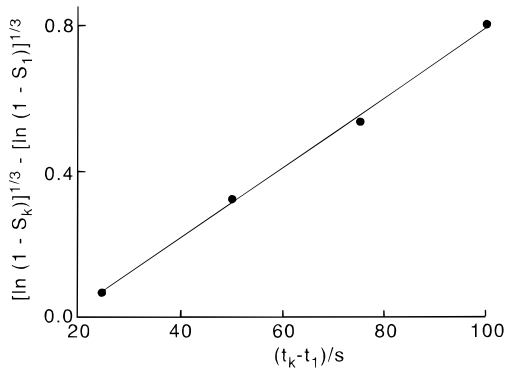

Figure 6. Application of eq 3 to the sequence of images shown in Figure 3.

monitoring of the absolute *z* piezo voltage during scanning.[9,10] The latter was recorded by scaling down the *z* piezo voltage using a potential divider and feeding it to an external input channel of the electronic control unit of the AFM, which permitted an absolute voltage map of the scanned area to be generated. Calibration of the voltage then permitted real drops or increases in height to be measured. This calibration was achieved by imaging a test grid, with a known precisely defined thickness of 2400 Å, and measuring the z piezo voltage changes between topographical maxima and minima. Using this procedure a voltage−height "conversion constant" of 0.308 V/μm was calculated. In this way the absolute height of the crystal could be measured throughout the reaction.

Commercially available *p*-chloranil (Aldrich, 99%) was employed without further purification. Single crystals of *p*-chloranil—up to approximately 1 cm in length—were grown using the slow cooling process[4] from saturated solutions of *p*-chloranil in toluene, seeded with smaller preselected crystals. The best results were obtained by slow cooling of the saturated solution from 55 °C to room temperature over periods of

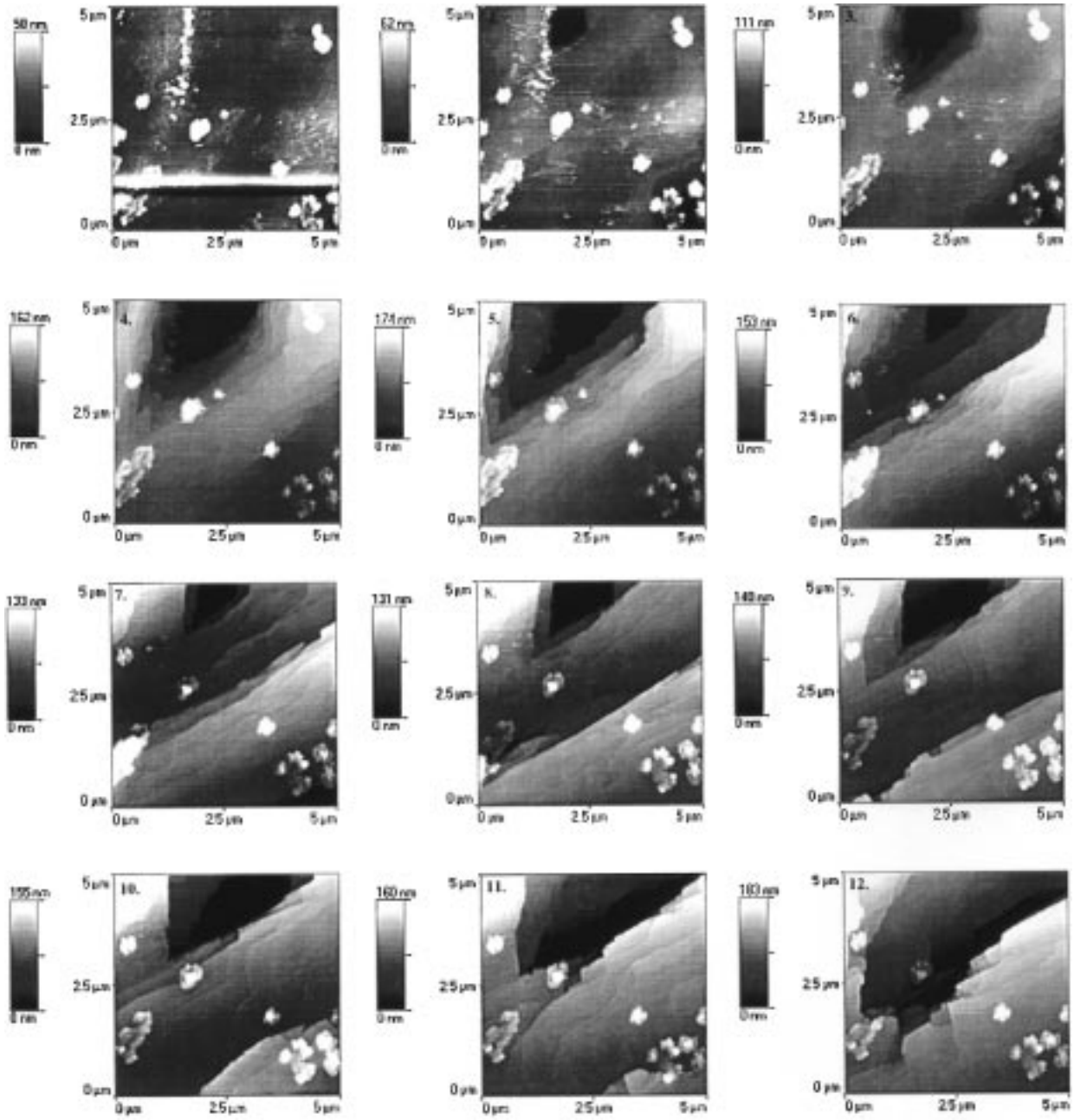

Figure 7. AFM sequence showing the effect of a solution containing 1.42 mM DMPA, 0.2 M KCl, and 15.9 mM KOH on a (010) surface of *p*-chloranil. The first image was taken ca. 150 s after solution changeover. Successive images were recorded at 25 s intervals.

between 168 and 300 h in a 500 mL crystal growing flask. The solution was kept in motion by a slowly rotating paddle to ensure solution homogeneity. The solution cooling rate was controlled by using a home-built programmable temperature water bath. It consisted of an electronic controlling system which triggered the illumination of a powerful light bulb (275 W IR reflector, GEC Electronics), which shone through one side of the water bath to provide heating. The largest crystals formed were approximately 0.7 × 0.7 × 0.3 cm in size. Suitably smaller sized crystals prepared in this way were characterized using X-ray diffraction techniques. The unit cell dimensions and the unit cell volume were in excellent agreement with literature.[11]

Potassium hydroxide and potassium chloride were both obtained from Aldrich as was *N*,*N*-dimethylphenylenediamine in the form of the hydrochloride salt (DMPA·2HCl; 99%). Solutions were made up using deionized water of resistivity 18 MΩ cm.

Results and Discussion

Atomic force microscopy was used to follow the evolution of (010) surfaces of *p*-chloranil when exposed to aqueous solutions containing DMPA with concentrations of up to ca. 10 mM. A typical series of images acquired immediately after the introduction of a solution of 4.87 mM DMPA, 23.8 mM KOH, and 0.2 M KCl onto a chloranil crystal is shown in Figure 3. Three observations can be made about the sequence. First the buildup of overgrowth occurs quite indiscriminately over the area examined, with no apparent preferred nucleation sites. Second the nucleation proceeds to give complete coverage of the substrate surface. This observation is emphasized by inspection of Figure 4 which shows a three-dimensional representation of the crystal surface after 9.5 min exposure. When complete coverage is attained, reaction ceases, as discussed below, and is confirmed by independent kinetic method using a channel flow cell.[12] Third the overgrowth occurs

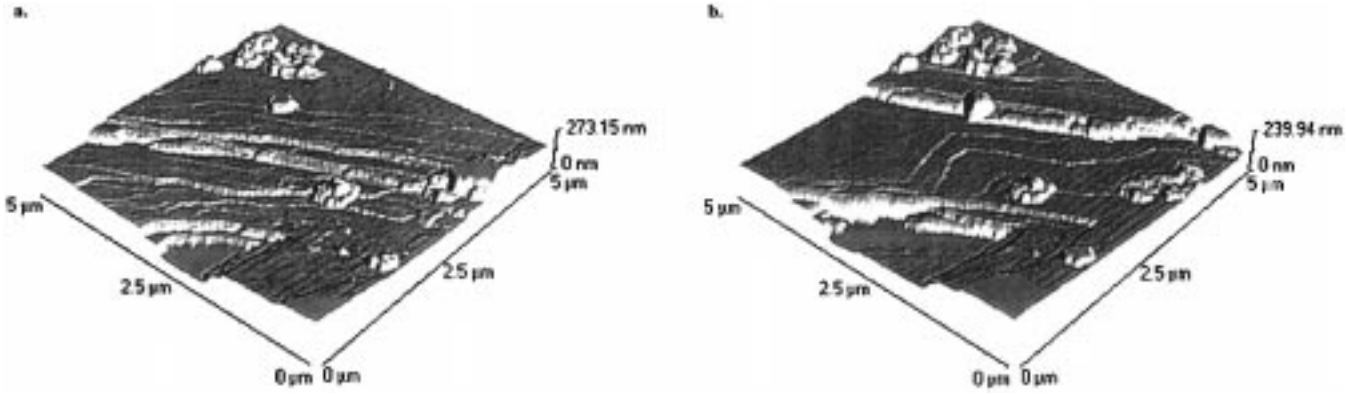

Figure 8. Three-dimensional renders of images 7 (a) and 9 (b) shown in Figure 7, highlighting the dominance of the alkaline dissolution process under the conditions employed.

in a progressive manner, in that more nuclei appear on the crystal surface as the exposure time increases.

The kinetics of the overgrowth nucleation were examined further by estimating the variation of the coverage of the crystal surface as a function of time. This was accomplished by taking line cross-sections at regular intervals across each image in a sequence, such as that in Figure 3. Fractional overgrowth coverages, $S(t)$, were calculated on the assumption that marked protrusions in the surface were growing nuclei and flat zones corresponded to fully reactive *p*-chloranil. The resulting data were analyzed by analogy with models developed for the growth of electrodeposited metal films[8,13,14] for which the time (t) dependence of S is given by

$$1 - S(t) = \exp(-k_n t^n) \tag{1}$$

where the exponent n reflects whether in the case of interest the passivation arises from the growth of nuclei formed instantaneously ($n = 2$) or progressively ($n = 3$), as schematically differentiated in Figure 5. The rate constant k_n/s^{-n} partly reflects the rate of growth of the enlarging nuclei, partly the number of nuclei per unit area, and, for $n = 3$, partly the rate of nucleation. In the "progressive" case the rate of nucleation is given by

$$\text{rate} = A't \tag{2}$$

where A' is a constant.

Because the time origin of the passivation sequences was a little ill-defined owing to the requirement for solution changeover in the AFM liquid cell to initiate reaction, the compatibility of eq 1 was examined by eliminating the absolute time as a variable as follows. Since the time differences between successive images are known, it is possible to relate data points in the sequence by subtraction of two equations of the form given for $S(t)$. This leads to the following equation

$$[\ln(1 - S_k)]^{1/3} - [\ln(1 - S_1)]^{1/3} = k_3 \Delta t \tag{3}$$

where Δt is the time interval between the kth and the first data point in the sequence. A typical plot based on eq 3 is shown in Figure 6 and corresponds to the series of images shown in Figure 3. The linearity of the plot displayed in Figure 6, and of other such plots, shows that eq 1 accurately describes the kinetics of overgrowth formation of the *p*-chloranil surface and that the passivating layer is formed from the coalescence of product nuclei progressively formed at a rate given by eq 2.

The onset of complete passivation of the crystal face was found to depend crucially on the concentration of DMPA in the solution. At relatively low concentrations (<2 mM) compared to KOH (typically ca. 15 mM), hydroxide-induced dissolution[4] was found to become dominant. This is clear in the sequence of images shown in Figure 7. Although there is evidence of some nucleation on the surface prior to the first topograph shown, this does not persist at longer times, when only dissolution appears to be significant. A clearer view of this is presented in Figure 8, which is three-dimensional renderings of the two images 7 and 9 in the sequence shown in Figure 7. As well as highlighting marked dissolution, Figure 8 shows that dissolution occurs without the displacement of the nuclei resident on the chloranil surface. This suggests that the latter are strongly attached to the surface.

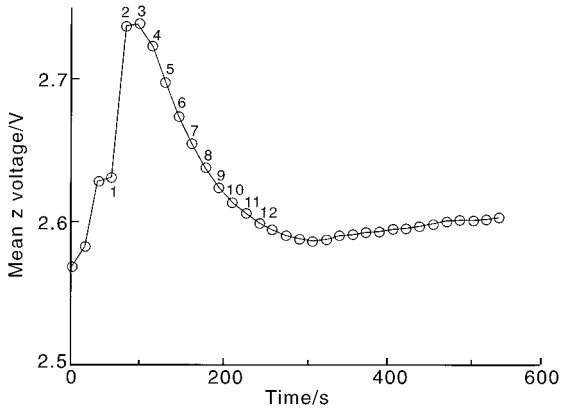

Figure 9. Plot of the mean z piezo voltage as a function of time corresponding to the AFM sequence shown in Figure 3. The numbered points apply to the corresponding image in the latter.

The topograpical data discussed above were acquired in tandem with z piezo voltage data (see Experimental Section). A typical (surface averaged) z piezo versus time profile is plotted in Figure 9, where the data correspond to the particular sequence shown in Figure 3. The data points corresponding to the 12 images shown in the latter are numbered as such. The profile shows, over the first 600 s following the introduction of the amine solution into the fluid cell, a clear increase to a maximum, followed by a decrease to a steady value. The initial rise in the mean z voltage suggests that over this time period there is a net dissolution. This conclusion is supported by the absence of significant overgrowth on the chloranil surface observed in images 1 and 2 of the topographical sequence shown in Figure 3. The fall in voltage after the maximum corresponds to surface growth and is consistent with the accumulation of the insoluble material seen in images 3−12 of Figure 3. The leveling off in the plot beyond image 12 is consistent with the observation that

the surface has become completely covered, and therefore largely inert toward reaction with the amine containing solution.

Quantification of the slope of the decaying portion of plots such as that shown in Figure 9 provides a direct measure of the mean (surface averaged) growth rate of the passivation product in a direction normal to the chloranil surface. In the example shown the maximum slope is 1.2×10^{-3} V s^{-1} corresponding to a normal growth rate of 4.4 nm s^{-1}. Corresponding measurements made for different concentrations of DMPA in the range 2−10 mM showed surprisingly little variation, indicating that the growth rate normal to the surface was largely independent of the DMPA concentration. This observation suggests that the rate determining step of the amination reaction may involve the release of chloranil from the solid.

Conclusions

The kinetics of passivation of *p*-chloranil by reaction with alkaline aqueous DMPA as characterized by atomic force microscopy may be parametrized by means of a surface coverage of overgrowth evolving in time as predicted by eq 1 with $n = 3$ corresponding to progressive nucleation. *z* piezo measurements show that before significant passivation is realized, dissolution of the solid takes place.

The approach described above provides a means of studying and kinetically characterizing solid/liquid reactions in which there is self-passivation resulting from the insolubility of the reaction product. In particular the applicability of equations derived for the formation of metal films at interfaces from nucleation and growth models is noted.

Acknowledgment. We thank the EPSRC for support via ROPA, Zeneca plc, and the EPSRC for a CASE studentship for J.B. and Giles Sanders for assistance with some of the AFM measurements.

References and Notes

(1) Atherton, J. H. *Res. Chem. Kinet.* **1996**, *2*, 193.
(2) Compton, R. G.; Harding, M. S.; Atherton, J. H.; Brennan, C. M. *J. Phys. Chem.* **1993**, *97*, 4677.
(3) Tam, K. Y.; Compton, R. G.; Atherton, J. H.; Brennan, C. M.; Docherty, R. *J. Am. Chem. Soc.* **1996**, *118*, 4419.
(4) Booth, J.; Sanders, G. H. W.; Compton, R. G.; Atherton, J. H.; Brennan, C. M. *J. Electroanal. Chem.* **1998**, *440*, 83.
(5) Booth, J.; Hong, Q.; Compton, R. G.; Prout, C. K.; Payne, R. M. *J. Colloid Interface Sci.* **1997**, *192*, 207.
(6) Renfrew, A. H. M. *Rev. Prog. Color. Relat. Top.* **1985**, *15*, 15.
(7) Chambers, J. Q. In *The Chemistry of the Quinoid Compounds*; Patai, S., Ed.; John Wiley and Sons: New York, 1988; pp 719−757.
(8) Harrison, J. A.; Thirsk, H. R. *Electroanal. Chem.* **1971**, *5*, 67.
(9) Sanders, G. H. W.; Booth, J.; Compton, R. G. *Langmuir* **1997**, *13*, 3080.
(10) Hong, Q.; Suárez, M. F.; Coles, B. A.; Compton, R. G. *J. Phys. Chem.* **1997**, *101*, 5557.
(11) van Weperen, K. J.; Visser, G. J. *Acta Crystallogr.* **1972**, *B28*, 338.
(12) Booth, J. Ph.D. thesis, University of Oxford, 1996.
(13) Evans, U. R. *Trans. Faraday Soc.* **1945**, *41*, 365.
(14) Abyaneh, M. Y. *J. Electroanal. Chem.* **1995**, *387*, 29, and references cited therein.